

Distributed phase-covariant cloning with atomic ensembles via quantum Zeno dynamics

Li-Tuo Shen¹, Huai-Zhi Wu^{1,*} and Zhen-Biao Yang²

¹*Department of Physics, Fuzhou University, Fuzhou 350002, People's Republic of China*

²*Key Laboratory of Quantum Information, University of Science and Technology of China, CAS, Hefei 230026, P. R. China*
(Dated: August 22, 2018)

We propose an interesting scheme for distributed orbital state quantum cloning with atomic ensembles based on the quantum Zeno dynamics. These atomic ensembles which consist of identical three-level atoms are trapped in distant cavities connected by a single-mode integrated optical star coupler. These qubits can be manipulated through appropriate modulation of the coupling constants between atomic ensemble and classical field, and the cavity decay can be largely suppressed as the number of atoms in the ensemble qubits increases. The fidelity of each cloned qubit can be obtained with analytic result. The present scheme provides a new way to construct the quantum communication network.

PACS numbers: PACS number:

I. INTRODUCTION

Quantum information processing via quantum Zeno dynamics [1] is a fascinating feature in quantum communication network, which is different from the quantum Zeno effect (QZE) [2, 3]. The most remarkable practical application of quantum Zeno dynamics is to suppress decoherence and dissipation via frequent measurements, which build a Zeno subspace that the system can evolve in [4, 5]. Until now, protocols about generating entanglement and implementing the quantum logic gate via quantum Zeno dynamics have been proposed [6–11], and the QZE has been experimentally observed in various systems [12–14], such as cavity QED [13] and Bose-Einstein condensates [14]. On the other hand, Pellizzari [15] first proposed a scheme to realize the reliable transfer of quantum information in two distant cavities connected by an optical fiber in 1997, which provides an essential tool for long-distant quantum communication schemes in recent years [16–24]. Yin and Li [17] generalized the idea to the atomic ensemble case, where the operation time of quantum computation can be greatly speeded up, however, the scheme is based on the coherently dynamical evolution which is more sensitive to the effects of spontaneous emission of atoms and photon leakage out of cavity. Unfortunately, there is still no report about distributed quantum computation via quantum Zeno dynamics with the atomic ensembles.

Another distinguishing feature of quantum system is quantum state cloning, which is first proved by Wootters and Zurek [25] as the no-cloning theorem that based on the linearity of quantum mechanics. However, a lot of research about approximate quantum state cloning has been proposed [26–35]. Many experimental realizations of quantum state cloning have also been done [36–41]. But the proposal about distributed quantum state cloning is still not reported.

To avoid the defects that decoherence is a main influence in the previous system taking one atom as a qubit, and to take full advantages of the atomic ensembles in reducing the effect of dissipation, we propose a scheme for distributed quantum state cloning with atomic ensembles via quantum Zeno dynamics. Compared with the previous schemes with only one atom as a qubit, the distinct features of our scheme are as follows: (1) The entanglement of the atomic ensembles is very robust against cavity decay and the distributed orbital state quantum cloning can be realized with only one step without auxiliary qubit. (2) The coupling strength between the atom and cavity can be collectively enhanced as the number of the atoms in each cavity increases, but the operation time prolongs much slowly. Thus, the demand on the rigorous condition of large coupling strength between single atom and cavity field becomes not so high in our scheme. (3) The quantum state cloning can be controlled by adjusting classical laser at different nodes. The present scheme can also be generalized to other systems, such as superconducting quantum interference device [42] and nitrogen vacancy center [43]. This kind of quantum cloning is important tools for studying a wide variety of task, such as state estimation [44], quantum cryptography [45] and distributed measurements [46], and provides a very new way for the quantum communication network in future.

*Electronic address: huaizhi.wu@fzu.edu.cn

II. MODEL

The quantum Zeno dynamics is governed by the Hamiltonian $H_K = H + KH_m$, where H is the Hamiltonian of the quantum system to be investigated and H_m can be considered as an additional interaction Hamiltonian performing the measurement. K stands for coupling constant. The subsystem of interest is governed by the evolution operator $U(t) = \lim_{K \rightarrow \infty} \exp(iKH_m t)U_K(t)$ when a strong coupling limit $K \rightarrow \infty$, which has the form $U(t) = \exp(-it \sum_n P_n H P_n)$ and P_n represents the eigenprojection of the H_m corresponding to the eigenvalue λ_n ($H_m = \sum_n \lambda_n P_n$) [4, 5]. Thus the limiting evolution operator $U_K(t) \sim \exp(-iKH_m t)U(t) = \exp[-i \sum_n (K\lambda_n P_n + P_n H P_n)t]$, so that the effective Hamiltonian can be written as $H_{eff} = \sum_n (K\lambda_n P_n + P_n H P_n)$, which is an important result in the quantum Zeno dynamics.

As shown in Fig. 1 (a), we consider that the atomic ensembles are trapped in each of the distant cavities connected by a $1 \times N$ ($N \geq 3$) single-mode integrated optical star coupler [49, 50], where each atomic ensemble consists of M identical three-level atoms. The optical star coupler is made up of N identical optical fiber channels and only one resonant field mode interacts with the cavity mode which possesses the ability for present quantum information processing. Under the rotating-wave approximation, the Hamiltonian of the whole system in the interaction picture reads

$$\begin{aligned} H_{total} &= H_{laser} + H_I, \\ H_{laser} &= \sum_{x=1}^N \sum_{i=1}^M \Omega_x |e_{i,x}\rangle \langle f_{i,x}| + H.c., \\ H_I &= \sum_{x=1}^N \sum_{i=1}^M (g_x a_x |e_{i,x}\rangle \langle g_{i,x}| + v_x b^+ a_x) + H.c., \end{aligned} \quad (1)$$

where H_{laser} plays a role of the Hamiltonian to be investigated and H_I acts as an additional interaction Hamiltonian performing the measurement in quantum Zeno dynamics. Here, the notation $|K_{i,x}\rangle$ ($K = e, f, g$) represents atom i with the state $|K\rangle$ in cavity x . The transition $|f_{i,x}\rangle \leftrightarrow |e_{i,x}\rangle$ is resonantly driven by the classical laser field with the Rabi frequency Ω_x , the atomic transition $|g_{i,x}\rangle \leftrightarrow |e_{i,x}\rangle$ is resonantly coupled to the field mode of the x th cavity with the coupling constant g_x . a_x (b) and a_x^+ (b^+) are the annihilation and creation operators for the x th cavity field (the field mode of the optical fiber channel), and v_x is the coupling strength of the x th cavity mode to the field mode of the optical fiber channel. We assume the parameters $g_x = g$, $v_x = v$ and $\Omega_{x'} = \Omega$ ($x' = 2, 3, \dots, N$) for simplicity. The interaction between atomic ensemble and cavity field is collectively enhanced leading to a energy splitting of $2\sqrt{M}g$, as shown in Fig. 1 (b). The driving laser at the transition resonant frequency ω is detuning from the both dressed states. In consequence, the atom-cavity system is only perturbed by the classical field driving if the driving strength is weak enough comparing with the energy splitting, which is the fundamental principle of the quantum Zeno dynamics. For convenience, in the following we take the expression $|A_f, B_g, C_e\rangle_x$ ($A, B, C = 0, 1, 2, \dots$) that denotes the state of atomic ensemble, where there are A atoms, B atoms and C atoms in the ground state $|f\rangle$, $|g\rangle$ and $|e\rangle$ of each atom in the x th cavity, respectively. $|1, M-1, 0\rangle_x$ denotes the symmetric superposition of the states for which only one atom is in $|f\rangle$ and the other in $|g\rangle$ in the x th atomic ensemble, i.e., the W state [32].

Assume that the first ensemble is initially in the W state and all the atoms in other ensembles are initially in $|g\rangle$. The initial state of the whole system is

$$\begin{aligned} |\Phi(0)\rangle &= |1_f, M-1_g, 0\rangle_1 \otimes \prod_{\xi=2}^N |0_f, M_g, 0_e\rangle_\xi \\ &\otimes \prod_{i=1}^N |0\rangle_i \otimes |0\rangle_f, \end{aligned} \quad (2)$$

Thus, the system will evolve in the subspace

$$\begin{aligned} \mathcal{L} &= \left\{ (|\phi_1\rangle, |\phi_2\rangle, |\phi_3\rangle), |\phi_4\rangle, (|\phi_5\rangle, |\phi_6\rangle, |\phi_7\rangle), \right. \\ &\quad \left. (|\phi_8\rangle, |\phi_9\rangle, |\phi_{10}\rangle), \dots, (|\phi_{3N-1}\rangle, |\phi_{3N}\rangle, |\phi_{3N+1}\rangle) \right\} \\ &\equiv \left\{ (|1_f, M-1_g, 0_e\rangle_1 |0\rangle_1, |0_f, M-1_g, 1_e\rangle_1 |0\rangle_1, \right. \\ &\quad \left. |0_f, M_g, 0_e\rangle_1 |1\rangle_1) \otimes \prod_{i=2}^N |0_f, M_g, 0_e\rangle_i |0\rangle_i \otimes |0\rangle_f, \right\} \end{aligned}$$

$$\begin{aligned}
& \prod_{i=1}^N |0_f, M_g, 0_e\rangle_i |0\rangle_i \otimes |1\rangle_f, \\
& (|0_f, M_g, 0_e\rangle_2 |1\rangle_2, |0_f, M - 1_g, 1_e\rangle_2 |0\rangle_2, \\
& |1_f, M - 1_g, 0_e\rangle_2 |0\rangle_2) \otimes \prod_{i=1, i \neq 2}^N |0_f, M_g, 0_e\rangle_i |0\rangle_i \otimes |0\rangle_f, \\
& (|0_f, M_g, 0_e\rangle_3 |1\rangle_3, |0_f, M - 1_g, 1_e\rangle_3 |0\rangle_3, \\
& |1_f, M - 1_g, 0_e\rangle_3 |0\rangle_3) \otimes \prod_{i=1, i \neq 3}^N |0_f, M_g, 0_e\rangle_i |0\rangle_i \otimes |0\rangle_f, \\
& \dots, \\
& (|0_f, M_g, 0_e\rangle_N |1\rangle_N, |0_f, M - 1_g, 1_e\rangle_N |0\rangle_N, \\
& |1_f, M - 1_g, 0_e\rangle_N |0\rangle_N) \otimes \prod_{i=1}^{N-1} |0_f, M_g, 0_e\rangle_i |0\rangle_i \otimes |0\rangle_f \}.
\end{aligned} \tag{3}$$

Under the condition of quantum Zeno dynamics $\Omega, \Omega_1 \ll g, v$, the whole Hilbert subspace is split into different invariant Zeno subspaces, the eigenprojection of H_I is $P_n^\alpha = |\alpha\rangle\langle\alpha|$ ($n = 1, 2, 3, \dots, 3N + 1$), where $|\alpha\rangle$ is the corresponding eigenstate of H_I in the whole subspace. If the corresponding eigenvalue is λ_n , then the effective Hamiltonian reads [5]

$$\begin{aligned}
H_{total} & \simeq \sum_{n, \alpha, \beta} (\lambda_n P_n^\alpha + P_n^\alpha H_{laser} P_n^\beta) \\
& = \sum_{n, \alpha} \lambda_n P_n^\alpha + H_e,
\end{aligned} \tag{4}$$

$$\begin{aligned}
H_e & = \frac{v}{\sqrt{Nv^2 + Mg^2}} \left(\Omega_1 |\phi_1\rangle\langle\phi_2| \right. \\
& \quad \left. + \Omega \sum_{k=2}^N |\phi_{3k+1}\rangle\langle\phi_2| + H.c. \right),
\end{aligned} \tag{5}$$

where

$$|\phi_2\rangle = \frac{v}{\sqrt{Nv^2 + Mg^2}} (|\phi_2\rangle - \frac{\sqrt{Mg}}{v} |\phi_4\rangle + \sum_{k=2}^N |\phi_{3k}\rangle), \tag{6}$$

after an interaction time t , the state of the system becomes

$$\begin{aligned}
|\Phi(t)\rangle & = \left[\frac{\Omega_1}{\Omega} + \frac{(N-1)\Omega}{\Omega_1} \right]^{-1} \left\{ \left[\frac{\Omega_1}{\Omega} \cos(\mu t) \right. \right. \\
& \quad \left. \left. + \frac{(N-1)\Omega}{\Omega_1} \right] |\phi_1\rangle + \left[\cos(\mu t) - 1 \right] \sum_{k=2}^N |\phi_{3k+1}\rangle \right. \\
& \quad \left. - i \frac{\sqrt{\Omega_1^2 + (N-1)\Omega^2}}{\Omega} \sin(\mu t) |\phi_2\rangle \right\},
\end{aligned} \tag{7}$$

where $\mu = \left(v \sqrt{\Omega_1^2 - \Omega^2 + N\Omega^2} \right) / \sqrt{Nv^2 + Mg^2}$. If we set $t = (2n+1) \pi / \mu$ ($n = 0, 1, 2, \dots$) and $\Omega_1 = (\sqrt{N} + 1)\Omega$, then the system will become

$$\begin{aligned}
|\Phi(t)\rangle & = \frac{1}{\sqrt{N}} \left(|\phi_1\rangle + \sum_{k=2}^N |\phi_{3k+1}\rangle \right) \\
& = \frac{1}{\sqrt{N}} \left(|1_f, M - 1_g, 0_e\rangle_1 |0_f, M_g, 0_e\rangle_2 \right. \\
& \quad \left. |0_f, M_g, 0_e\rangle_3 \dots |0_f, M_g, 0_e\rangle_N \right. \\
& \quad \left. + |0_f, M_g, 0_e\rangle_1 |1_f, M - 1_g, 0_e\rangle_2 \right)
\end{aligned}$$

$$\begin{aligned}
& \left(|0_f, M_g, 0_e\rangle_3 \dots |0_f, M_g, 0_e\rangle_N \right. \\
& + |0_f, M_g, 0_e\rangle_1 |0_f, M_g, 0_e\rangle_2 \\
& + |1_f, M - 1_g, 0_e\rangle_3 \dots |0_f, M_g, 0_e\rangle_N \\
& + \dots \\
& + |0_f, M_g, 0_e\rangle_1 |0_f, M_g, 0_e\rangle_2 \\
& \left. + |0_f, M_g, 0_e\rangle_3 \dots |1_f, M - 1_g, 0_e\rangle_N \right) \\
& \otimes \prod_{i=1}^N |0\rangle_i \otimes |0\rangle_f. \tag{8}
\end{aligned}$$

Therefore the coupling strength between the atom and cavity can be collectively enhanced to $\sqrt{M}g$, but the operation time prolongs much slowly. Therefore, we obtain the W state of the atomic ensembles in N separate cavities. It should be noted that the key step to achieve the orbital state quantum cloning is to prepare the W state of the atomic ensembles [32]. For this reason, it is necessary to consider the feasibility for generating the W state of the atomic ensemble qubits. In the above derivations, we assume the condition of quantum Zeno dynamics $\Omega_1, \Omega \ll g', v$, therefore, we take the influence of the ratios $\Omega/(\sqrt{M}g)$ and $v/(\sqrt{M}g)$ on the fidelity of the W state of atomic ensemble into consideration, as shown in Fig. 2 (a). The result shows that the fidelity decreases in an oscillating form with the increase in the ratio of Ω/g' and keeps higher than 90% even when $\Omega = 0.1\sqrt{M}g$ and $v = 0.5\sqrt{M}g$, hence our scheme can work well in a large scale of feasible numbers for v and Ω . In Fig. 2 (b), We plot the fidelity F versus the dimensionless parameters $\kappa/(\sqrt{M}g)$, $\gamma/(\sqrt{M}g)$ and $\beta/(\sqrt{M}g)$, where γ, κ, β are, respectively, the decay rates for the spontaneous emission of atom in each cavity and photon leakage out of each cavity and the optical fiber channel. The result indicates that the dominant factor of reducing the fidelity is the atomic spontaneous emission, and the fidelity is almost unaffected by the decay of the cavity even when $\kappa = 0.01\sqrt{M}g$. If we fix the parameter g , the ratio $\Omega/(\sqrt{M}g)$, $\kappa/(\sqrt{M}g)$, $\gamma/(\sqrt{M}g)$ and $\beta/(\sqrt{M}g)$ all become tunable by choosing the suitable parameter M , which is simpler and more feasible under the current experiment condition. We also consider the main experiment setups to implement the distributed quantum state cloning. The fiber-based high-finesse cavity parameters $(g', \kappa, \gamma)/2\pi = (185, 53, 3)\text{MHz}$ have been reported in the recent experiment [33]. When the optical fiber loss factor at the 852nm wavelength is 2.2 dB km⁻¹ [34], corresponding to the decay rate $\beta = 0.15\text{MHz}$. In a general case in the present scheme, for example $M = 100$, then the real coupling constant g between each atom and the cavity is only 18.5MHz, so that $v = 0.5\sqrt{M}g = 90\text{MHz}$ which is not so large in experiment. With decoherence of the quantum system, the distributed multi-atom W states generation scheme can be obtained with a high fidelity larger than 97.66% when $N = 3$, and the interaction time t needed to complete the operation is 0.147us. The deviation $|\delta g'| = 0.1g'$ only reduces the fidelity by about 10^{-2} when $N = 3$, where $g' = \sqrt{M}g$ and the deviation may be induced by the number of atoms in each cavity or the coupling strength between single atom and the cavity.

Based on the previously prepared W state, the quantum cloning scheme is now able to be implemented. Again, we assume that all the cavities and the optical fiber channel are initially both in the vacuum state, and only one atom of the first cavity is prepared in the arbitrary orbital state of the Bloch sphere [35]

$$|\psi\rangle = \cos\left(\frac{\theta}{2}\right)|g\rangle + \sin\left(\frac{\theta}{2}\right)e^{i\delta}|f\rangle, \tag{9}$$

where the angle θ is a known parameter, but δ is unknown to us, and the other atoms are initially in the ground states $|g\rangle$. We assume that the first ensemble is initially in the superposition of $|0, M, 0\rangle$ and $|1, M - 1, 0\rangle$ and all the atoms in other ensembles are initially in $|g\rangle$. Thus the whole system is initially prepared in the state

$$\begin{aligned}
|\Psi(0)\rangle & = \left(\cos\left(\frac{\theta}{2}\right)|0_f, M_g, 0_e\rangle_1 + \sin\left(\frac{\theta}{2}\right)e^{i\delta}|1_f, M - 1_g, 0_e\rangle_1 \right) \\
& \otimes \prod_{\xi=2}^N |0_f, M_g, 0_e\rangle_\xi \otimes \prod_{i=1}^N |0\rangle_i \otimes |0\rangle_f. \tag{10}
\end{aligned}$$

The state $\prod_{i=1}^N |0_f, M_g, 0_e\rangle_i |0\rangle_i \otimes |0\rangle_f$ undergoes no changes because the corresponding effective Hamiltonian $H'_e = 0$ in the quantum Zeno dynamics. On the other hand, the state $|1_f, M - 1_g, 0_e\rangle_1 \otimes \prod_{\xi=2}^N |0_f, M_g, 0_e\rangle_\xi \otimes \prod_{i=1}^N |0\rangle_i \otimes |0\rangle_f$ will evolve in the subspace \mathcal{L} .

The effective reduced density operators ρ_{eff}^1 of qubit 1 and ρ_{eff}^2 of qubit 2 are

$$\rho_{eff}^1 = \cos^4\left(\frac{\theta}{2}\right) + |A(t)|^2 \sin^4\left(\frac{\theta}{2}\right) + \cos^2\left(\frac{\theta}{2}\right) \sin^2\left(\frac{\theta}{2}\right)$$

$$\begin{aligned} & \left[(N-1)(|B(t)|^2 + |C(t)|^2) \right. \\ & \left. + |D(t)|^2 + A(t) + A^\dagger(t) \right], \end{aligned} \quad (11)$$

$$\begin{aligned} \rho_{eff}^2 = & \cos^4\left(\frac{\theta}{2}\right) + |B(t)|^2 \sin^4\left(\frac{\theta}{2}\right) + \cos^2\left(\frac{\theta}{2}\right) \sin^2\left(\frac{\theta}{2}\right) \\ & \left[(N-2)(|B(t)|^2 + |C(t)|^2) + |A(t)|^2 \right. \\ & \left. + |C(t)|^2 + |D(t)|^2 + B(t) + B^\dagger(t) \right], \end{aligned} \quad (12)$$

where

$$\begin{aligned} A(t) &= \left[\frac{\Omega_1}{\Omega} + \frac{(N-1)\Omega}{\Omega_1} \right]^{-1} \left[\frac{\Omega_1}{\Omega} \cos(\mu t) + \frac{(N-1)\Omega}{\Omega_1} \right], \\ B(t) &= \left[\frac{\Omega_1}{\Omega} + \frac{(N-1)\Omega}{\Omega_1} \right]^{-1} \left[\cos(\mu t) - 1 \right], \\ C(t) &= -i \sin(\mu t) \frac{\sqrt{\Omega_1^2 + (N-1)\Omega^2}}{\Omega} \frac{v}{\sqrt{Nv^2 + Mg^2}}, \\ D(t) &= i \sin(\mu t) \frac{\sqrt{\Omega_1^2 + (N-1)\Omega^2}}{\Omega} \frac{\sqrt{Mg}}{\sqrt{Nv^2 + Mg^2}}, \end{aligned} \quad (13)$$

and other effective reduced density operator ρ_{eff}^j for qubit j ($j \geq 3$) is exactly the same with that of qubit 2, this is because the encoding in qubit 2 is the exactly symmetry to that in qubit j , therefore we just focus on the qubit 1 that is to be cloned and qubit 2 that has been cloned in the following discussions. Set $t' = \pi\sqrt{Nv^2 + g^2} / \left(v\sqrt{\Omega_1^2 - \Omega^2 + N\Omega^2} \right)$ and $\Omega_1 = (\sqrt{N} + 1)\Omega$, the whole system becomes

$$\begin{aligned} |\Psi(t')\rangle &= \left[\cos\frac{\theta}{2} \prod_{i=1}^N |0_f, M_g, 0_e\rangle_i + \sin\frac{\theta}{2} e^{i\delta} \frac{1}{\sqrt{N}} \right. \\ & \left(|1_f, M-1_g, 0_e\rangle_1 |0_f, M_g, 0_e\rangle_2 \right. \\ & |0_f, M_g, 0_e\rangle_3 \dots |0_f, M_g, 0_e\rangle_N \\ & + |0_f, M_g, 0_e\rangle_1 |1_f, M-1_g, 0_e\rangle_2 \\ & |0_f, M_g, 0_e\rangle_3 \dots |0_f, M_g, 0_e\rangle_N \\ & + |0_f, M_g, 0_e\rangle_1 |0_f, M_g, 0_e\rangle_2 \\ & |1_f, M-1_g, 0_e\rangle_3 \dots |0_f, M_g, 0_e\rangle_N \\ & + \dots \\ & \left. + |0_f, M_g, 0_e\rangle_1 |0_f, M_g, 0_e\rangle_2 \right. \\ & \left. |0_f, M_g, 0_e\rangle_3 \dots |1_f, M-1_g, 0_e\rangle_N \right) \\ & \otimes \prod_{i=1}^N |0\rangle_i \otimes |0\rangle_f, \end{aligned} \quad (14)$$

the corresponding fidelity of each cloned qubit reads

$$\begin{aligned} F &= \cos^4\frac{\theta}{2} + \frac{1}{N} \sin^4\frac{\theta}{2} \\ & + \left(\frac{N-1}{N} + \frac{2}{\sqrt{N}} \right) \cos^2\frac{\theta}{2} \sin^2\frac{\theta}{2}, \end{aligned} \quad (15)$$

where $\theta \in [0, \pi/2]$. For the case $\theta = \pi/2$ and $N = 3$, we obtain the optimal fidelity of the $1 \rightarrow 3$ phase-covariant cloning [32], therefore we construct a $1 \rightarrow N$ distributed orbital state quantum cloning machine with only one step.

Our derivation for the effective reduced density operators of different qubit is based on the quantum Zeno dynamics. To check the validity of the result, we numerically simulate the effective model in Eq. (11) and Eq. (12), and the full Hamiltonian model in Fig. 3 (a). We also plot the evolutions for reduced density operators of the effective model and

full model with different experimental parameters θ , M , N versus gt respectively from Fig. 3 (b) to Fig. 3 (g). The result shows that the smaller the θ , the fidelity of all copies is higher and fluctuates less in the system evolution, and the operation time is proportional to \sqrt{M} in Fig. 3 (b) and (c). The tendencies in Fig. 3 (d) and (e) indicate that the more the number of atoms M in each cavity, the time needed to reach the optimal fidelity of all copies becomes longer. The plots of Fig. 3 (f) and (g) demonstrate that the result of the quantum cloning become bad as the number of copies N increases. Fig. 4 shows the influences of different fluctuations on the fidelity F of the cloned qubit 2 when $N = 3$. Particularly, F versus the errors of the interaction time t and the fluctuations in θ are plotted in Fig. 4 (g), the result shows that the optimal fidelity of cloned qubit 2 is almost unaffected even when the relative fluctuations in t and θ are both about 10%. 10% deviations in other different parameters only reduces the fidelity by about 10^{-2} . The reason is that our quantum state cloning is dependent on the evolution of the W state. However, the fidelity is independent of the phase factor δ which makes the quantum state cloning workable. Therefore, the distributed quantum cloning based on quantum Zeno dynamics is robust against fluctuations of different experiment parameters.

III. EXPERIMENT FEASIBILITY AND CONCLUSION

Now we give a detailed discussion of the experimental feasibility and this secular setup. The atomic configuration involved in our scheme can be implemented with a cesium atom [51]. For $7s_{1/2}$ of the cesium atom, we have $r_g \approx 2.6nm$ and $d \approx 4.1M^{-1/2}\mu m$, where the no-direct-interaction condition can be satisfied very well when $M < 200$. Thus, all the atoms in the cavity have the nearly same coupling strength and collectively interact with the cavity field [17]. Single cesium atom can be localized at a fixed position in each cavity with a high precision for a long time [52]. The near-perfect cavity-fiber coupling with an efficiency larger than 99.9% has been reported [53], and a technique of using a $1 \times N$ star fiber optic coupler as a distributed strain sensor in a white-light interferometer is presented [54]. The star coupler is realized as in [55] by using a planar arrangement of two confocal arrays of radial waveguides performing with efficiency approaching 100% under ideal conditions, when the waveguides have strong mutual couplings. Finally, N resonant classical laser fields are applied to each atom within an appropriate operation time, which plays the role of the “ external fields ” for the quantum Zeno dynamics. In fact, we do not think of g and v as free control parameters which can be made arbitrarily “ large ”, but fix the parameters g and v during the evolution of the system, and take the condition that g and v are both infinitely strong just as an approximation [5], compared to Ω . Even when the condition $\Omega \ll g, v$ is not well satisfied, i.e., the system does not evolve via quantum Zeno dynamics, the fidelity of the entanglement also keeps very high. For example, even when $\Omega = 0.1\sqrt{M}g = 18.5MHz$ and $v = 0.1\sqrt{M}g = 18.5MHz$, the fidelity of the entanglement is 87.37%.

In conclusion, we have proposed a scheme to implement the distributed orbital state quantum cloning with atomic ensembles via quantum Zeno dynamics. The quantum cloning can be achieved via appropriate coupling of atomic ensemble qubits at different nodes. Therefore, the present scheme provides a new way to construct an atomic ensemble quantum network via quantum Zeno dynamics using the single-mode integrated optical star coupler, which is very robust against cavity decay and very promising to be realized with current experiment technology.

IV. ACKNOWLEDGEMENTS

L.T.S. and H.Z.W acknowledge support from the Major State Basic Research Development Program of China under Grant No. 2012CB921601, National Natural Science Foundation of China under Grant No. 10974028, the Doctoral Foundation of the Ministry of Education of China under Grant No. 20093514110009, and the Natural Science Foundation of Fujian Province under Grant No. 2009J06002. Z.B.Y is supported by the National Basic Research Program of China under Grants No. 2011CB921200 and No. 2011CBA00200, and the China Postdoctoral Science Foundation under Grant No. 20110490828.

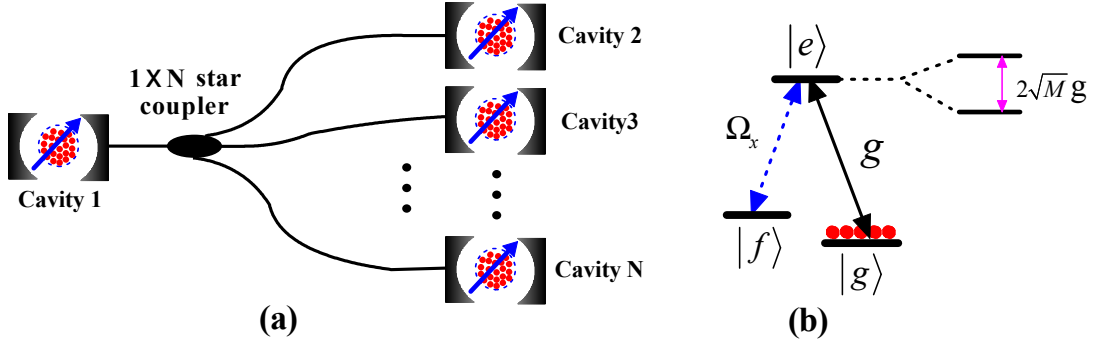


FIG. 1: (Color online) (a) The experimental setup for implementing the distributed orbital state quantum cloning with atomic ensembles. M identical three-level atoms are trapped in N distant cavities respectively, and these cavities are connected by a $1 \times N$ single-mode integrated optical star coupler. Each blue solid in each cavity represents a classical laser on each atomic ensemble, which keeps invariant during the whole quantum Zeno dynamical evolution. (b) Configuration of the equivalent atomic ensemble level structure and relevant transitions. The states $|g\rangle$ and $|f\rangle$ correspond to two ground state of the atomic ensemble, and $|e\rangle$ is the excited state. $2\sqrt{M}g$ is the energy space between the dressed states of the excited state $|e\rangle$ when the number of the atoms in the corresponding atomic ensemble is M .

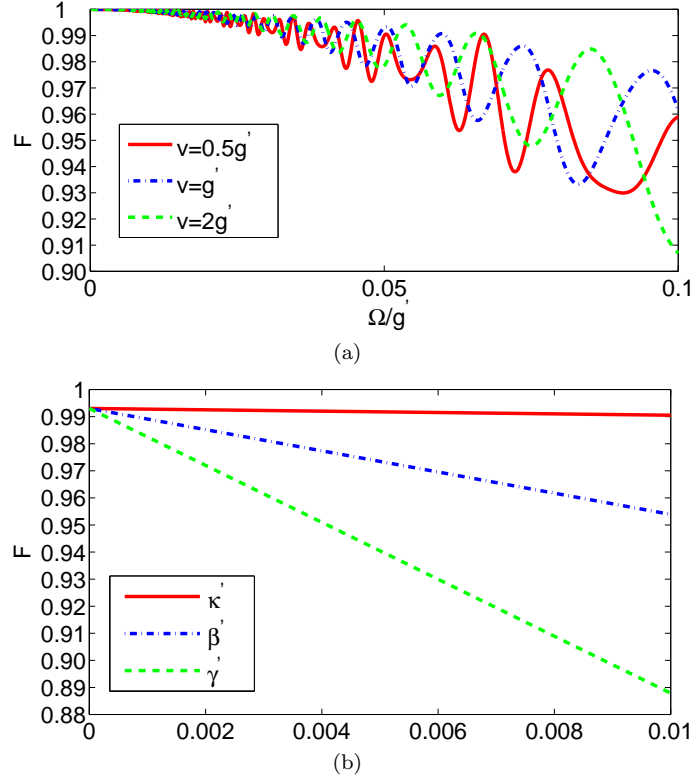


FIG. 2: (Color online) The fidelity F of the entanglement between the atomic ensembles versus different parameters when $N = 3$. (a) F versus different ratios Ω/g' when $v = 0.5g'$ (the red solid line), g' (the blue dot dash line) and $2g'$ (the green dash line), where $g' = \sqrt{M}g$. (b) F versus $\kappa' = \kappa/(\sqrt{M}g)$ (the red solid line), $\beta' = \beta/(\sqrt{M}g)$ (the blue dot dash line), and $\gamma' = \gamma/(\sqrt{M}g)$ (the green dash line).

-
- [1] P. Facchi, V. Gorini, G. Marmo, S. Pascazio, and E. C. G. Sudarshan, Phys. Lett. A **275**, 12 (2000).
 [2] B. Misra and E. C. G. Sudarshan, J. Math. Phys. **18**, 756 (1977).
 [3] W. M. Itano, D. J. Heinzen, J. J. Bollinger, and D. J. Wineland, Phys. Rev. A **41**, 2295 (1990).
 [4] P. Facchi and S. Pascazio, Phys. Rev. Lett. **89**, 080401 (2002).

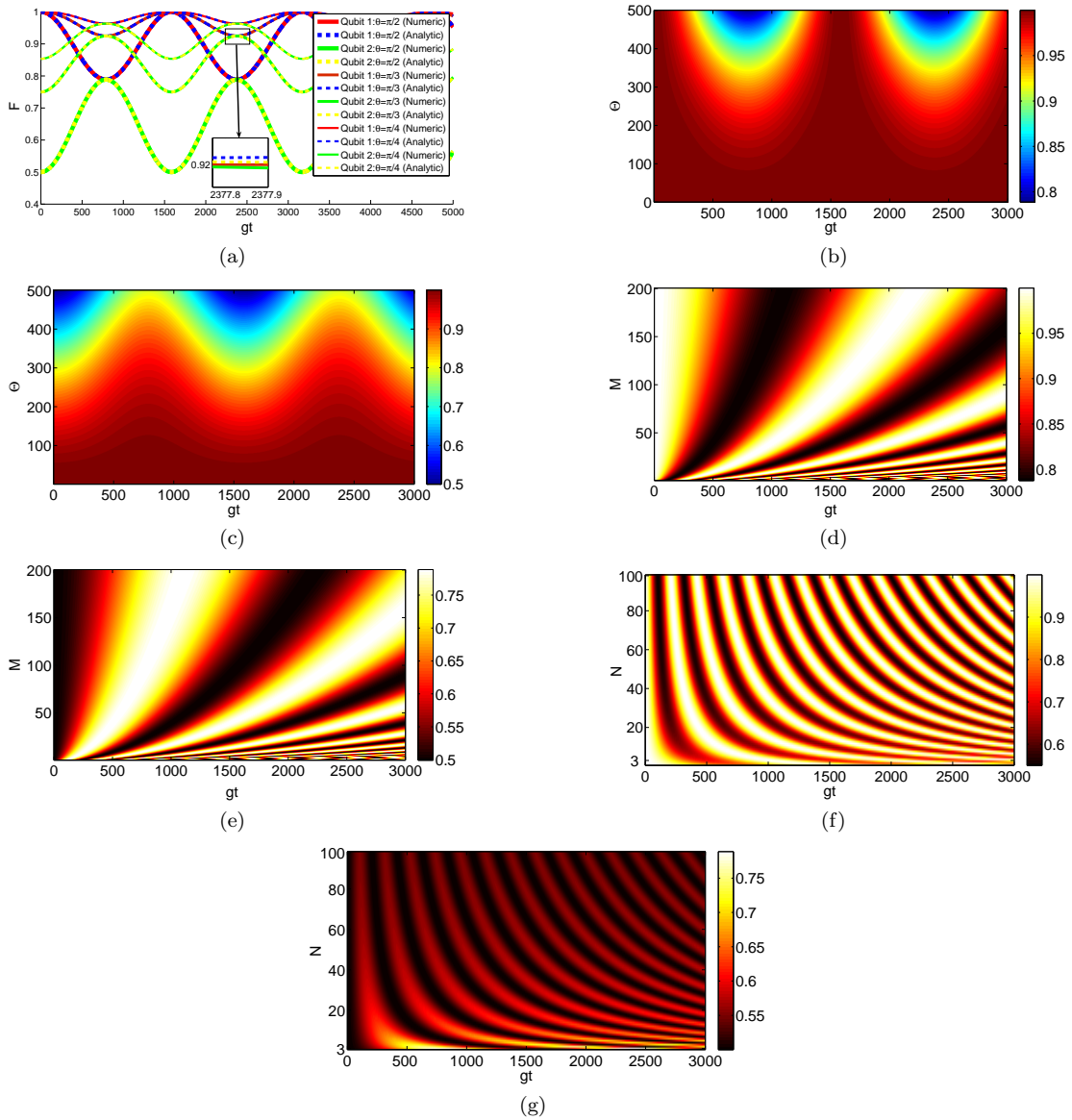


FIG. 3: (Color online) The effective model is plotted with dash lines and the full dynamics is plotted with solid lines. (a) The fidelity F of different cloned qubits versus the dimensionless parameter gt with $N = 3$ and $M = 100$. (b) The fidelity F of qubit 1 versus parameters Θ ($\Theta = 1000\theta/\pi$) and gt . (c) The fidelity F of qubit 2 versus parameters Θ ($\Theta = 1000\theta/\pi$) and gt . (d) The fidelity F of qubit 1 versus parameters M and gt with $\theta = \pi/2$ and $N = 3$. (e) The fidelity F of qubit 2 versus parameters M and gt with $\theta = \pi/2$ and $N = 3$. (f) The fidelity F of qubit 1 versus parameters N and gt with $\theta = \pi/2$ and $M = 100$. (g) The fidelity F of qubit 2 versus parameters N and gt with $\theta = \pi/2$ and $M = 100$.

- [5] P. Facchi, G. Marmo, and S. Pascazio, J. Phys: Conf. Ser. **196**, 012017 (2009).
- [6] Y. P. Huang and M. G. Moore, Phys. Rev. A **77**, 062332 (2008).
- [7] H. Azuma, Phys. Rev. A **68**, 022320 (2003).
- [8] C. R. Myers and A. Gilchrist, Phys. Rev. A **75**, 052339 (2007).
- [9] X. Q. Shao, L. Chen, S. Zhang, Y. F. Zhao, and K. H. Yeon, Eur. Phys. Lett. **90**, 50003 (2010).
- [10] X. Q. Shao, H. F. Wang, L. Chen, S. Zhang, Y. F. Zhao, and K. H. Yeon, Phys. Rev. A **80**, 062323 (2009).
- [11] W. A. Li and G. Y. Huang, Phys. Rev. A **83**, 022322 (2011).
- [12] R. J. Cook, Phys. Scr. T **21**, 49 (1988).
- [13] J. Bernu, S. Deléglise, C. Sayrin, S. Kuhr, I. Dotsenko, M. Brune, J. M. Raimond, and S. Haroche, Phys. Rev. Lett. **101**, 180402 (2008).
- [14] E. W. Streed, J. Mun, M. Boyd, G. K. Campbell, P. Medley, W. Ketterle, and D. E. Pritchard, Phys. Rev. Lett. **97**, 260402 (2006).
- [15] T. Pellizzari, Phys. Rev. Lett. **79**, 5242 (1997).

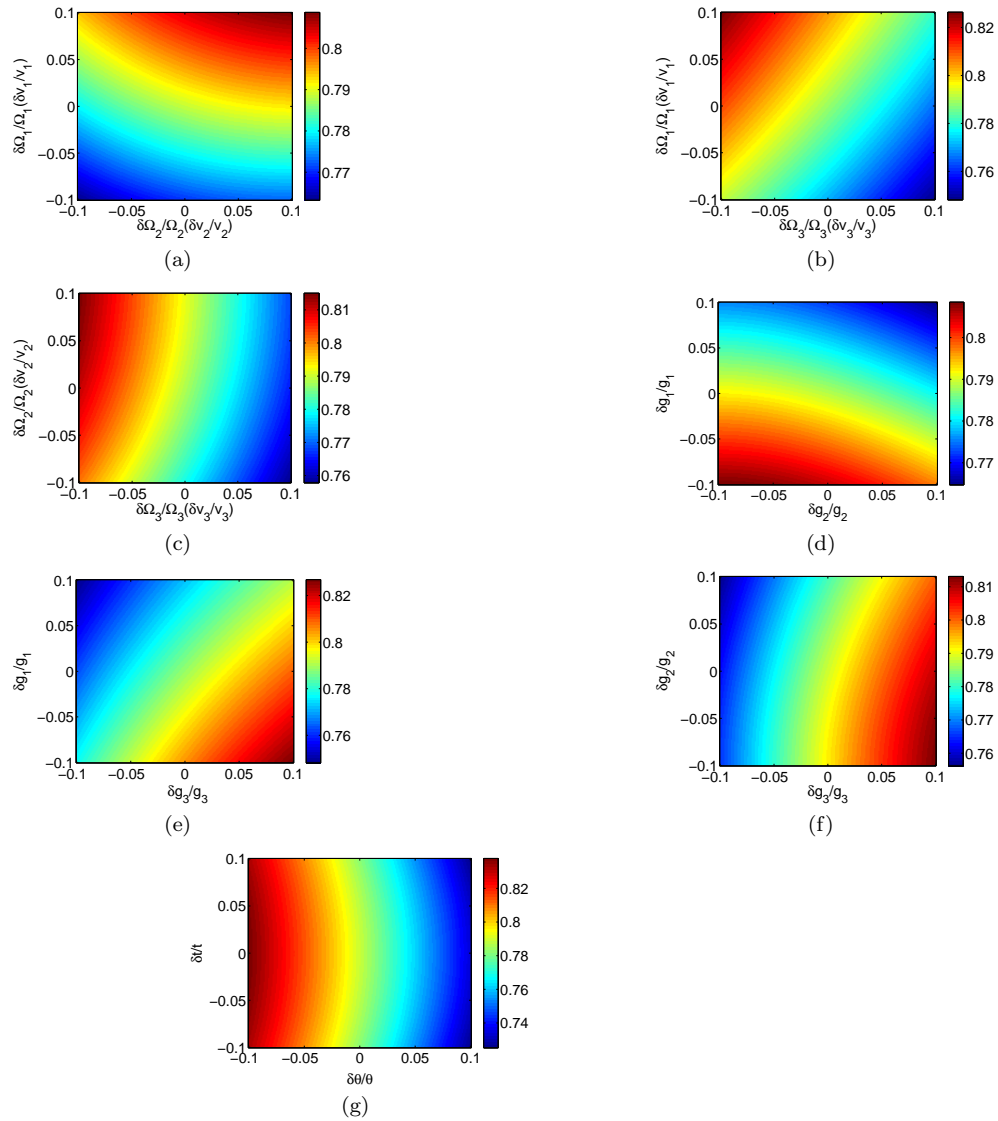


FIG. 4: (Color online) The fidelity F of the cloned qubit 2 versus various fluctuations of the experiment parameters. All subfigures are plotted with the parameter $N = 3$, $\Omega = 0.05\sqrt{M}g$, $v = 0.5g$ and $\theta = \pi/2$, therefore the optimal fidelity is 0.788. $g_1 = g_2 = g_3 = \sqrt{M}g$. (a) F vs $\frac{\delta\Omega_1(\delta v_1)}{\Omega_1(v_1)}$ and $\frac{\delta\Omega_2(\delta v_2)}{\Omega_2(v_2)}$; (b) F vs $\frac{\delta\Omega_1(\delta v_1)}{\Omega_1(v_1)}$ and $\frac{\delta\Omega_3(\delta v_3)}{\Omega_3(v_3)}$; (c) F vs $\frac{\delta\Omega_2(\delta v_2)}{\Omega_2(v_2)}$ and $\frac{\delta\Omega_3(\delta v_3)}{\Omega_3(v_3)}$; (d) F vs $\frac{\delta g_1}{g_1}$ and $\frac{\delta g_2}{g_2}$; (e) F vs $\frac{\delta g_1}{g_1}$ and $\frac{\delta g_3}{g_3}$; (f) F vs $\frac{\delta g_2}{g_2}$ and $\frac{\delta g_3}{g_3}$; (g) F vs $\frac{\delta t}{t}$ and $\frac{\delta \theta}{\theta}$;

- [16] S. B. Zheng, Appl. Phys. Lett. **90**, 154101 (2009).
- [17] Z. Q. Yin and F. L. Li, Phys. Rev. A **75**, 012324 (2007).
- [18] A. Serafini, S. Mancini, and S. Bose, Phys. Rev. Lett. **96**, 010503 (2006).
- [19] Z. B. Yang, H. Z. Wu, W. J. Su, and S. B. Zheng, Phys. Rev. A **80**, 012305 (2009).
- [20] S. Y. Ye, Z. R. Zhong, and S. B. Zheng, Phys. Rev. A **77**, 014303 (2008).
- [21] S. B. Zheng, C. P. Yang, and F. Nori, Phys. Rev. A **82**, 042327 (2010).
- [22] P. Peng and F. L. Li, Phys. Rev. A **75**, 062320 (2007).
- [23] J. Song, Y. Xia, H. S. Song, J. L. Guo, and J. Nie, Eur. Phys. Lett. **80**, 60001 (2007).
- [24] D. Bruß, G. M. D'Ariano, M. Lewenstein, C. Macchiavello, A. Sen(De), and U. Sen, Phys. Rev. Lett. **93**, 210501 (2004).
- [25] W. K. Wootters and W. H. Zurek, Nature (London) **299**, 802 (1982).
- [26] D. Bruß, M. Cinchetti, G. M. D'Ariano, and C. Macchiavello, Phys. Rev. A **62**, 012302 (2000).
- [27] H. Fan, K. Matsumoto, X. B. Wang, and M. Wadati, Phys. Rev. A **65**, 012304 (2001).
- [28] G. M. D'Ariano and C. Macchiavello, Phys. Rev. A **67**, 042306 (2003).
- [29] R. F. Werner, Phys. Rev. A **58**, 1827 (1998).
- [30] V. Bužek and M. Hillery, Phys. Rev. A **54**, 1844 (1996).

- [31] N. Gisin and S. Massar, Phys. Rev. Lett. **79**, 2153 (1997).
- [32] S. B. Zheng, J. Opt. B: Quantum Semiclassical Opt. **7**, 139 (2005).
- [33] J. Volz, R. Gehr, G. Dubois, J. Estève, and J. Reichel, Nature **475**, 210 (2011).
- [34] K. J. Gordon, V. Fernandez, P. D. Townsend, and G. S. Buller, IEEE J. Quantum Electron. **40**, 900 (2004).
- [35] A. T. Rezakhani, S. Siadatnejad, and A. H. Ghaderi, Phys. Lett. A **336**, 278 (2005).
- [36] A. Lamas-Linares, C. Simon, J. C. Howell, and D. Bouwmeester, Science **296**, 712 (2002).
- [37] H. K. Cummins, C. Jones, A. Furze, N. F. Soffe, M. Mosca, J. M. Peach, and J. A. Jones, Phys. Rev. Lett. **88**, 187901 (2002).
- [38] J. F. Du, T. Durt, P. Zou, H. Li, L. C. Kwek, C. H. Lai, C. H. Oh, and A. Ekert, Phys. Rev. Lett. **94**, 040505 (2005).
- [39] H. W. Chen, D. W. Lu, B. Chong, G. Qin, X. Y. Zhou, X. H. Peng, and J. F. Du, Phys. Rev. Lett. **106**, 180404 (2011).
- [40] M. Sabuncu, U. L. Andersen, and G. Leuchs, Phys. Rev. Lett. **98**, 170503 (2007).
- [41] E. Nagali, D. Giovannini, L. Marrucci, S. Slussarenko, E. Santamato, and F. Sciarrino, Phys. Rev. Lett. **105**, 073602 (2010).
- [42] J. P. Cleuziou *et al.*, Nature **1**, 53 (2006).
- [43] P. Neumann, *et al.*, Nature **6**, 249 (2010).
- [44] D. Bruss, A. Ekert and C. Macchiavello Phys. Rev. Lett. **81**, 2598 (1988).
- [45] A. K. Ekert, Phys. Rev. Lett. **67**, 661 (1991).
- [46] D. Bruß, J. Calsamiglia and N. Lütkenhaus Phys. Rev. A **63**, 042308 (2001).
- [47] L. Bartůšková, M. Dušek, A. Černoč, J. Soubusta, and J. Fiurášek, Phys. Rev. Lett. **99**, 120505 (2007).
- [48] S. B. Zheng and G. C. Guo, Phys. Rev. A **73**, 032329 (2006).
- [49] T. Findakly and B. Chen, Appl. Phys. Lett. **40**, 549 (1982).
- [50] F. H. L. E. Herbert, and T. Kurnio, Jpn. J. Appl. Phys. **36**, 5136 (1997).
- [51] A. Boca, R. Miller, K. M. Birnbaum, A. D. Boozer, J. McKeever, and H. J. Kimble, Phys. Rev. Lett. **93**, 233603 (2004).
- [52] J. McKeever, J. R. Buck, A. D. Boozer, A. Kuzmich, H. C. Nagerl, D. M. Stamper-Kurn, and H. J. Kimble, Phys. Rev. Lett. **90**, 133602 (2003).
- [53] S. M. Spillane, T. J. Kippenberg, O. J. Painter, and K. J. Vahala, Phys. Rev. Lett. **91**, 043902 (2003).
- [54] L. B. Yuan and L. M. Zhou, Appl. Opt. **90**, 4168 (1998).
- [55] C. Dragone, C. H. Henry, I. P. Kaminow, and R. C. Kistler, IEEE Photon. Technol. Lett. **1**, 241 (1989).